Modelling Dual Pathways for the Metazoan Spindle Assembly Checkpoint

Richard P. Sear[1] and Martin Howard[2]

[1]*Department of Physics, University of Surrey, Guildford, Surrey GU2 7XH, UK.*
[2]*Department of Mathematics, Imperial College London,*
South Kensington Campus, London SW7 2AZ, UK.
(Dated: February 4, 2008)

Using computational modelling, we investigate mechanisms of signal transduction focusing on the spindle assembly checkpoint where a single unattached kinetochore is able to signal to prevent cell cycle progression. This inhibitory signal switches off rapidly once spindle microtubules have attached to all kinetochores. This requirement tightly constrains the possible mechanisms. Here we investigate two possible mechanisms for spindle checkpoint operation in metazoan cells, both supported by recent experiments. The first involves the free diffusion and sequestration of cell-cycle regulators. This mechanism is severely constrained both by experimental fluorescence recovery data and also by the large volumes involved in open mitosis in metazoan cells. Using a simple mathematical analysis and computer simulation, we find that this mechanism can generate the inhibition found in experiment but likely requires a two stage signal amplification cascade. The second mechanism involves spatial gradients of a short-lived inhibitory signal that propagates first by diffusion but then primarily via active transport along spindle microtubules. We propose that both mechanisms may be operative in the metazoan spindle assembly checkpoint, with either able to trigger anaphase onset even without support from the other pathway.

Keywords: Signal transduction, kinetochore, spindle assembly checkpoint, mathematical modelling

The question of how a signal emanating from a small, compact structure in a cell can be amplified and propagated to an entire cell is fundamental to cell biology [1]. An excellent example is provided by the spindle assembly checkpoint (SAC) [2], which regulates cell cycle progression from metaphase to anaphase during mitosis. The segregation of sister chromatids that occurs during anaphase is permitted only after all the kinetochores are attached via microtubules to the mitotic spindle. Even a single unattached kinetochore can signal to the rest of the cell and prevent cell cycle progression [3, 4]. A fundamental issue is how a relatively small structure, such as a kinetochore, can generate sufficient signal to robustly communicate with distant subcellular locations [1]. Moreover, this signal must switch off rapidly, within a period of minutes, after complete kinetochore attachment to spindle microtubules [4]. These requirements strongly constrain the possible signal transduction mechanisms. In this paper, we focus particularly on the SAC in cases where the nuclear envelope breaks down prior to SAC activity (open mitosis), as in metazoan cells. In this context, we examine two distinct models: a diffusive sequestration model and a model involving active signal transport along spindle microtubules. We believe that both of these pathways may be in simultaneous operation in the metazoan SAC.

The metaphase/anaphase transition is triggered by an intricate sequence of events centred around the proteins securin, cyclin B and separase. The first step is the ubiquitination of securin and cyclin B by the Anaphase Promoting Complex/Cyclosome (APC/C) [5], a process that tags securin/cyclin B for destruction via the 26S proteasome. This degradation allows separase to cleave the cohesin complex that tethers sister chromatids together. Once the cohesin complex has been cleaved, the sister chromatids aree pulled apart to opposite poles by the mitotic spindle. In order to prevent premature entry into anaphase, the SAC must prevent securin/cyclin B ubiquitination by the APC/C until proper attachment of *all* chromosomes to the spindle. Evidence has accumulated for a number of overlapping, and therefore possibly redundant, mechanisms for SAC operation. The APC/C is known to be stimulated by Cdc20 binding; hence, a plausible way to achieve APC/C inhibition is to inhibit the ability of Cdc20 to bind to the APC/C. One possibility is that Cdc20 is held, sequestered, in an inactive form via binding to Mad2, with the production of Cdc20-Mad2 being promoted by unattached kinetochores [6, 7, 8]. Key proteins identified at unattached kinetochores include Bub1, Mad1, Mad2, BubR1 (Mad3 in budding yeast), Bub3 and Cdc20. Moreover, FRAP experiments have revealed that some of these proteins, including Mad2, BubR1 and Cdc20, turnover rapidly at unattached kinetochores [6, 9]. Furthermore, the available evidence suggests that Mad2 exists in two forms: open (O-Mad2) and closed (C-Mad2) [10, 11], with the closed form adopted when bound to Cdc20. Production of C-Mad2-Cdc20 may be catalysed via the kinetochore bound C-Mad2-Mad1 complex. Intriguingly, Refs. [7, 8] propose that C-Mad2-Cdc20 away from the unattached kinetochore can convert further cytosolic O-Mad2 and Cdc20 into their bound C-Mad2-Cdc20 state. In this way the relatively weak signal coming from an unattached kinetochore can be amplified leading to comprehensive Cdc20 sequestration throughout the cell. Recent experiments have further implicated a protein called p31[comet] in

switching off this signal after complete kinetochore attachment [7, 12, 13].

However, the above "Mad template" model is not the only proposed mechanism for APC/C repression. BubR1 and Bub3 are also known to bind Cdc20 and thus repress the APC/C [14]. Indeed, BubR1 appears to be a more potent inhibitor of Cdc20 than Mad2, and both BubR1 and Mad2 may mutually promote each other's binding to Cdc20 [15]. Furthermore, Bub1 is believed to phosphorylate Cdc20, possibly also repressing the APC/C [16]. In addition, the overall copy number of Cdc20 is down-regulated until all the kinetochores are attached [17]. Clearly, reducing the overall number of Cdc20 will impair the effectiveness of the APC/C prior to anaphase. Moreover, not only does Cdc20 form complexes with Mad2 and BubR1, but it is also believed to form a separate complex called the Mitotic Checkpoint Complex (MCC), consisting of Mad2, BubR1, Bub3 and Cdc20 [18]. This complex also appears to be a potent inhibitor of the APC/C [18]. In addition, the APC/C is regulated by phosphorylation through the kinase Cdk1 [19]. Lastly, the APC/C itself has intriguing localization properties, localizing, for example, to unattached kinetochores [20]. This positioning may also have implications for the mechanism of APC/C inhibition.

Recently, a pioneering paper by Doncic *et al.* [21] introduced a careful mathematical analysis to the question of how the SAC functions. Focusing on yeast, they analysed various simplified models of how an unattached kinetochore can signal to the rest of the cell. Yeast undergoes closed mitosis, where even at the onset of anaphase the nuclear envelope is still complete. As a consequence, a diffusive signal from an unattached kinetochore is only required to propagate within the nuclear volume of a few cubic microns. However, one important difference between yeast and metazoan cells is that the latter undergo open mitosis, where the nuclear envelope has broken down by the time the SAC is active; hence any freely diffusing signal from an unattached kinetochore must propagate throughout the cytoplasm, a volume a thousand times larger than the nucleus of a yeast cell. Furthermore a considerable amount of data is available concerning the metazoan SAC in the form of flourescent bleaching data and estimates for the copy numbers of the relevant molecules. In this paper, we therefore use computational modelling to analyze the SAC in metazoan cells. We develop a new model that incorporates two step signal amplification, a mechanism with close similarities to previously investigated multistep signal cascades [22, 23]. This similarity points towards a close connection between the SAC and other cell signalling systems, such as MAPK cascades. Importantly, we find that our model generates robust inhibition in metazoan cells, unlike models without an amplification step.

As discussed above, the most popular models of APC/C inhibition involve transport solely by diffusion. However, these models are hard to reconcile with experiments of Rieder *et al.* [24]. Using cells with two independent spindles, Rieder *et al.* found that unattached kinetochores on one spindle did not block anaphase onset in a neighbouring complete spindle. This experiment appears to indicate that any "wait anaphase" signal would have to be limited to a single spindle, and *not* diffuse throughout the cytosol. This finding is in clear contradiction with the mechanisms introduced above. For this reason we develop a second model where a short-lived signal from an unattached kinetochore first diffuses to a nearby microtubule, before being actively transported along spindle microtubules. In this way the signal is restricted to the spindle. Moreover, we propose that both the active transport and diffusive mechanisms may be in simultaneous use in metazoan cells. We suggest that either of the signalling mechanisms may individually be able to initiate anaphase, even without support from the other pathway. With this assumption, our models are then fully consistent with both the experiments of Rieder *et al.* [24] and with a diffusive sequestration model [7].

Results

Mechanisms with diffusive transport

We analyze the case where the kinetochores control the concentration of a freely diffusing species c. When a kinetochore is unattached and so is signalling, a large majority of the species c is in the c^* state, but when the last kinetochore itself switches off, the c^* species rapidly decays to the c state, thus communicating the switch-off (attachment) to the rest of the cell. We will sometimes refer to the c^* species as being in the inhibiting state as it is this state that prevents securin/cyclin B ubiquitination by the APC/C.

The concentrations of the freely diffusing species are almost uniform The timescale for diffusion across the cell is $\tau_D = r_c^2/D$, whereas the mean time for a molecule to collide with the kinetochore is $\tau_C = r_c^3/(Dr_k)$. Here D is the diffusion constant for the protein; r_c is the distance across the cell (typically a few tens of microns); and $r_k \simeq 0.2\mu$m [25] is the radius of the kinetochore. If we assume that the lifetime for the inhibiting c^* species is much longer than τ_D then any gradient in its concentration will clearly be small. Furthermore, the timescale for diffusion across the cell is much smaller than that for collisions with the kinetochore, $\tau_D/\tau_C = r_k/r_c \ll 1$. Hence, each molecule of the c species criss-crosses the cell many times between kinetochore reactions and so gradients in its concentration

are also small in most of the cell. If, on the other hand, the lifetime of the inhibiting species is short with respect to τ_D, then its concentration will no longer be uniform and instead density gradients will form. This scenario will arise later on when we consider models with active transport. However, for longer lifetimes, we can model the inhibition using simple ordinary differential equations.

Inhibitor production only at a kinetochore In the simplest possible model, the inhibiting c^* species is produced only at unattached kinetochores. We denote the steady state rate of production of c^* at the final unattached kinetochore by J_{off}. In order to allow the inhibition to be switched off at the beginning of anaphase, the inhibiting c^* species must be unstable. We model this instability by a first-order decay $c^* \to c$, with rate constant α. Cdc20 is known to activate the APC/C and so trigger anaphase. Since both Mad2 and BubR1 are known to bind to Cdc20, we can tentatively identify c as Cdc20 while c^* is a Mad2-Cdc20 or BubR1-Cdc20 complex. As the kinetochore is such a small structure, we now address the question of whether the flux of c^* produced *only* at a single unattached kinetochore is sufficient to maintain inhibition. At steady state the fluxes on and off a kinetochore must be the same, i.e. $J_{\text{on}} = J_{\text{off}}$. Furthermore, at steady state, the rate of production of c^* at the last unattached kinetochore must equal its rate of decay, i.e. $J_{\text{off}} = \alpha N_c^*$, where N_c^* is the number of inhibiting c^* molecules. Experimental data, largely on marsupial PtK$_1$ and PtK$_2$ cells, gives estimates for many of the model parameters [6, 26]. From this data we will be able to estimate the value of N_c^* and see whether good inhibition can be obtained.

Experimental evidence for the flux J_{off} is available from FRAP (Fluorescence Recovery After Photobleaching) data for the recovery of fluorescence of checkpoint proteins at unattached kinetochores. This data provides a direct measure of dissociation rates. Together with an estimate of the copy number of each kinetochore bound protein, we can then derive the off flux J_{off}. For BubR1 the (fast phase, see [6]) FRAP half-life ($t_{1/2}$) is 3s, whereas for Mad2 the half-life is $10 - 20$s [6, 9], with a kinetochore occupancy N_k of about 1000 molecules for both [6]. This gives an off flux of about $J_{\text{off}} = N_k \ln 2/t_{1/2} \sim 1000 \times \ln 2/3 \sim 200 \ s^{-1}$ for BubR1 and $J_{\text{off}} \sim 50 \ s^{-1}$ for Mad2. Note that these fluxes are actually the maximum possible, as not all of the released molecules will be in the inhibiting form. The lifetime of the inhibiting species α^{-1} has not been directly measured. However, anaphase begins about 20 min after the last kinetochore becomes attached [4]. Clearly, the number of inhibiting c^* molecules must decrease dramatically over a period of no more than about 10 min, giving an upper bound of $\alpha^{-1} \sim 10$min, a value which is also consistent with the data of Ref. [27]. If we sum the fluxes of Mad2 and BubR1 and set $\alpha^{-1} = 10$ min, the number of molecules $N_{c*} = J_{\text{off}}\alpha^{-1} \simeq 150,000$. The total number of Cdc20 molecules is approximately $800,000$ [6]. Thus with the experimental fluxes and even assuming a decay rate as slow as is reasonable we find that at steady state a single kinetochore can only sequester approximately 20% of the Cdc20. Furthermore, if the lifetime of the inhibiting c^* molecules is shorter than supposed by our upper bound $\alpha^{-1} \sim 10$min, or if the flux J_{off} is lower, then an even smaller fraction will be in the inhibiting state. Hence, the formation of Mad2/Cdc20 and BubR1/Cdc20 complexes solely at an unattached kinetochore cannot maintain good inhibition.

The experimental FRAP data used in the above analysis was not specifically derived from the *final* unattached kinetochore. Potentially the final unattached kinetochore might have a higher turnover rate, thereby generating greater inhibition. We therefore develop a complementary approach to determine whether a reaction only at a single unattached kinetochore is *in principle* sufficient to sequester most of the Cdc20. We estimate the inhibition that would be generated if the on flux J_{on} at the kinetochore were maximised, i.e., diffusion limited with a diffusion constant D at the top of the range of the values measured *in vivo*. Diffusion constants in the cytoplasm of metazoan cells have typically yielded values in the range 1 to $30\mu\text{m}^2\text{s}^{-1}$ [28, 29, 30, 31]. Also, Howell *et al.* [6] found that a bleached spot of cytoplasmic GFP-Cdc20 0.8μm across recovered its fluorescence in less than 0.2s, implying a diffusion constant $\gtrsim 5\mu\text{m}^2\text{s}^{-1}$. If the on flux to the unattached kinetochore is diffusion limited, then using a plate geometry appropriate for a kinetochore, the on flux at steady state is given by $J_{\text{on}} \sim 4Dr_k N_c/v_c$ [32]. Here, N_c is the number of c molecules, $v_c = 6000\mu\text{m}^3$ is the cytoplasmic volume [6], and we use a fast diffusion constant $D = 30\mu\text{m}^2\text{s}^{-1}$. At steady state the flux J_{on} must be balanced by the $c^* \to c$ flux, $J_{c*\to c} = \alpha N_{c*}$. Equating these two fluxes and defining the constant total number of molecules as $N = N_c + N_{c*}$ (neglecting a negligible number at the kinetochore), we have $N_{c*}/N = (1 + \alpha v_c/4Dr_k)^{-1} \approx 3/4$. Hence, even in an optimistic scenario, only about three-quarters of the Cdc20 can be sequestered. Furthermore, to reach this limit, high flux rates are required, much higher than found experimentally for BubR1/Mad2 (see above). For these reasons, it is unlikely (though still theoretically possible) that the metazoan SAC could function through this method.

The fundamental difficulty with this mechanism can be presented in an alternative way that brings out the essential role played by the cell volume. The time each molecule spends in the c^* form is on the order of α^{-1}. The time taken for each molecule in the c state to find the unattached kinetochore is about v_c/k_k, where k_k is the unattached kinetochore binding rate. This time scale is proportional to the cell volume and hence becomes longer as the cell size increases. As the volume increases, for fixed lifetime α^{-1}, each molecule spends less and less time in the inhibiting state and

eventually the mechanism fails.

Autocatalysis One way to try to increase the number of inhibiting molecules would be for the reaction that sequesters Cdc20 to occur not just on the kinetochore but also off the kinetochore. If c^* itself catalyzes an off kinetochore $c \to c^*$ reaction then the reaction is autocatalytic. Autocatalysis was considered by Doncic *et al.* [21], where it was found to be unsatisfactory for the case of closed mitosis in yeast. The reason is that, for good inhibition, the off-kinetochore autocatalysis will likely have a large reaction rate, as the on-kinetochore reaction is on its own insufficient to maintain good inhibition (see above). Consequently, when the kinetochore reaction is switched off, the result is only a weak perturbation of an autocatalytic reaction. In other words inhibition of a "go anaphase" signal either cannot be switched off, or switches off only very slowly (see Fig. 1). Interestingly, the Mad2 template model proposed by Ref. [7] is essentially identical to this mechanism, where the closed form of Mad2 catalyzes the conversion of open to closed Mad2 both on and off the kinetochore. Thus an unattached kinetochore inhibits anaphase by generating C-Mad2-Cdc20 which in turn generates more C-Mad2-Cdc20 off the kinetochore via an autocatalytic reaction. However, by itself this autocatalytic mechanism does not allow switch off of the metazoan SAC for the same reason it does not for the SAC in yeast.

Autocatalysis could play a role in the inhibition, provided an additional process switches off the autocatalytic reaction once the last kinetochore attaches to a microtubule. It has been suggested that the protein p31$^{\mathrm{comet}}$ could play a role in this context [7, 12, 13]. Potentially p31$^{\mathrm{comet}}$ could be upregulated to abruptly switch off the SAC. However, the question is then how this signal could be turned on so rapidly after microtubule attachment to the final kinetochore. If p31$^{\mathrm{comet}}$ competes with O-Mad2 for C-Mad2 binding [13], then this is no easier than regulating the concentration of free Cdc20, our original problem. Potentially, p31$^{\mathrm{comet}}$ could be upregulated using a two step reaction process; however such a scheme would have to be conceptually similar to that discussed in the next section. We emphasize that p31$^{\mathrm{comet}}$ could also play other important roles, for example in switching off kinetochore signalling following microtubule attachment [33].

Model with an amplification step We now turn to a model with an off-kinetochore, but non-autocatalytic, reaction. This involves the species: e, e^* and c^*. We first assume that an e species cycles through the unattached kinetochore, where it is converted to the inhibiting e^* form. We further assume that the e^* is able to convert the e form to a second inhibiting c^* species, giving a second step to the signal amplification. Importantly the c^* form cannot convert further e into the c^* or e^* forms. This form of amplification ensures that only molecules that have passed through the unattached kinetochore participate in amplifying the inhibitory signal. As the inhibitory signal is not produced autocatalytically, it can switch off rapidly after the final kinetochore-microtubule attachment. The reaction processes are:

$$
\begin{aligned}
e + K &\xrightarrow{k_k} e^* + K & e^* &\xrightarrow{\alpha_e} e \\
e + e^* &\xrightarrow{k} c^* + e^* & c^* &\xrightarrow{\alpha} e,
\end{aligned}
\tag{1}
$$

where K is an unattached kinetochore. It is natural to associate the e species with free Cdc20, and the e^* and c^* species with complexes of Cdc20 such as C-Mad2-Cdc20 and BubR1-Cdc20. We are assuming that one form of the complex (e^*) can catalyze the production of further complexes (c^*) which differ in that the c^* cannot participate in manufacturing further complexes. This distinction between the two forms is a clear prediction of our modelling. However, we cannot definitively identify the difference between the c^* and e^* species, which could, for example, involve phosphorylation or a conformational change. Clearly, our reaction scheme is schematic; more complex schemes based on the same principles are certainly feasible. One possibility is that there could be more than two steps to the amplification process. Alternatively, p31$^{\mathrm{comet}}$ could be rapidly upregulated using a two step reaction, as discussed previously. Another possibility is using a two step reaction to modulate the decay rate α. Both possibilities could in principle lead to both good inhibition and rapid checkpoint switch off, but are fundamentally similar to the scheme of Eq. **1**. The key prediction of the model of Eq. **1** is for at least two species allowing non-autocatalytic amplification off the kinetochore and hence strong sequestration.

The above two-step process has close similarities to other multi-step signalling cascades such as for MAPK [22, 23]. However, there are differences, for example, the e species participates in both steps of the above amplification process. In MAPK cascades, on the other hand, a separate c species is converted to the c^* form in the second amplification reaction. Nevertheless, the principle of using more than one step to provide robust amplification but with rapid response times is similar and is likely conserved across many different signalling systems. However, the difficulty of robust signalling in the SAC is particularly acute, since the initial signal emerges from such a small region (a single unattached kinetochore).

For the parameter values of the reactions in Eq. **1**, we use $\alpha^{-1} = \alpha_e^{-1} = 5$min. These lifetimes are shorter than used previously: the two step nature of the reaction mechanism now dictates that shorter lifetimes are needed for switch off within the appropriate timeframe of less than 20 min. Despite these short lifetimes, a two step reaction cascade ensures that robust signal amplification is still achieved. In dilute solution *in vitro*, rate constants for diffusion-limited protein-protein association are around 10^{-3} to $10^{-2}\mu m^3 s^{-1}$ [34], with the exception of some large rate constants where there is significant electrostatic attraction between the proteins. We take an *in vivo* rate constant at the top end of these values, with $k = 10^{-2}\mu m^3 s^{-1}$. For the rate constant k_k, we use the diffusion limited value $k_k \sim 4Dr$ [32]. Assuming $D = 20\mu m^2 s^{-1}$, i.e. fairly fast cytoplasmic diffusion, we find $k_k \sim 20\mu m^3 s^{-1}$.

Since the gradients in the concentrations are small (see above), we can determine the time dependence and steady-state values of the three species from ordinary differential equations:

$$\frac{\mathrm{d}N_{e*}}{\mathrm{d}t} = \frac{k_k}{v_c}N_e - \alpha_e N_{e*}, \qquad \frac{\mathrm{d}N_{c*}}{\mathrm{d}t} = \frac{k}{v_c}N_{e*}N_e - \alpha N_{c*}, \tag{2}$$

$$\frac{\mathrm{d}N_e}{\mathrm{d}t} = -\frac{k_k}{v_c}N_e - \frac{k}{v_c}N_{e*}N_e + \alpha_e N_{e*} + \alpha N_{c*}, \tag{3}$$

where N_x is the number of molecules of species $x = e, e^*, c^*$. At steady state (ss), we have:

$$N_{e*}^{ss} = \frac{k_k}{v_c\alpha_e}N_e^{ss}, \qquad N_{c*}^{ss} = \frac{kk_k}{v_c^2\alpha\alpha_e}\left(N_e^{ss}\right)^2. \tag{4}$$
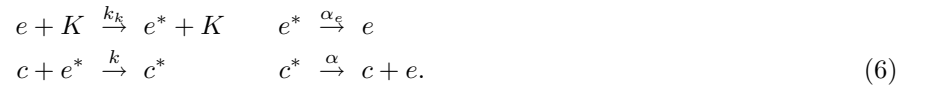
Defining the (constant) total number of molecules as $N = N_e + N_{e*} + N_{c*}$, we find:

$$N = \left(1 + \frac{k_k}{v_c\alpha_e}\right)N_e^{ss} + \frac{kk_k}{v_c^2\alpha\alpha_e}\left(N_e^{ss}\right)^2. \tag{5}$$

For $N = 800,000$, and using the above parameters, we find $N_e^{ss} \approx 40,000$, $N_{e*}^{ss} \approx 40,000$ and $N_{c*}^{ss} \approx 720,000$. Hence around 95% of the molecules are in the inhibiting state. For the single unattached kinetochore, we find that the diffusion limited on rate onto the kinetochore is about $J_{\mathrm{on}} \sim 4DrN_e^{ss}/v_c \sim 100s^{-1}$. Assuming a kinetochore population of around 1000, as found experimentally, this gives a half-life for the kinetochore bound population of $5 - 10$s. This is roughly consistent with the observed Mad2, BubR1 kinetochore half-lives [6, 9]. As shown in Fig. 1, we also find that the signal switches off quite quickly after microtubule attachment to the final kinetochore. After 10 min the fraction of the e molecules has increased from 5% to 24% and after 20 min 60% is in the e form. Moreover the switch-*on* of the checkpoint is even quicker, with good inhibition being reestablished within 1 min of even a single kinetochore detachment, see Fig. 1 inset. This is in good agreement with cyclin B1 data from Ref. [27], which suggests that switch-on is essentially an order of magnitude faster than SAC switch-off.

We therefore conclude that the above model is compatible with experiments. However, we did use a diffusion-limited value for k_k and a value of k near the top end of the range of reaction-rate constants for typical proteins in a dilute solution [34]. Reducing k by an order of magnitude weakens the level of inhibition, although over 85% of the molecules are still in the inhibiting state. However, the model is not consistent with experiments if the reaction rates are further reduced or if diffusion is substantially slowed. Thus we predict that if the mechanism of the SAC is diffusive amplified sequestration then measurements of the reaction rates will reveal rather fast reactions, or possibly more than two steps to the amplification process.

For completeness we also analyze an alternative two species model previously proposed by Doncic et al [21], for the smaller volumes involved in the yeast SAC. The reaction scheme for their model is:

$$\begin{array}{ll} e + K \xrightarrow{k_k} e^* + K & e^* \xrightarrow{\alpha_e} e \\ c + e^* \xrightarrow{k} c^* & c^* \xrightarrow{\alpha} c + e. \end{array} \tag{6}$$

Note that this scheme does not catalytically amplify the inhibitory signal. Here, one e^* molecule can only interact with one c molecule while in our previous model a single e^* molecule can convert many molecules into the inhibiting form, thereby producing amplification. For good inhibition we require $N_{e*}^{ss} + N_{c*}^{ss} \approx 800,000$. Using $\alpha^{-1} = \alpha_e^{-1} = 5$min, we find that the flux off the unattached kinetochore must be well over $1000s^{-1}$, faster than the diffusion limited maximum, even for high levels (10^5 copies) of the e species. This finding is, of course, not unexpected: the lack of amplification means that the flux of inhibitory molecules off the unattached kinetochore must be higher than in the catalytic model proposed above. We therefore believe that this model is probably not able to account for the SAC in metazoan cells.
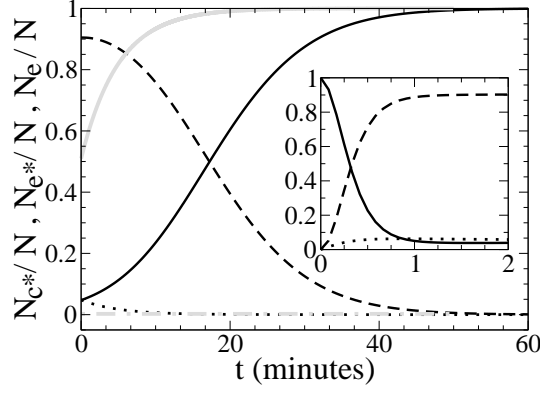
FIG. 1: Plot, for the model of Eq. **1**, showing the fraction of molecules N_e/N (solid line), N_{c*}/N (dashed line), N_{e*}/N (dotted line) as a function of time, with the final kinetochore attaching at time $t = 0$, i.e. initial steady-state concentrations, but k_k then set to zero at $t = 0$. Inset shows the same fractions, but starting with all N molecules in the e form and with k_k set to $20\mu m^3 s^{-1}$ at $t = 0$. For comparison, in the main plot, the fractions N_c/N for the production only at kinetochores and autocatalytic models are plotted as grey curves. They should be compared with the solid black curve. The grey solid curve is with a reaction only at a kinetochore, and the grey dot-dashed curve is with autocatalysis. Note that with a reaction only at a kinetochore the initial inhibition is weak whereas with autocatalysis inhibition is near total even when k_k is set to zero. The values of k (for the autocatalytic rate), α and k_k are the same in the single species models as for the model of Eq. **1**.

Mechanisms involving active transport

As shown above, our model with an amplification step is able to explain many features of the metazoan SAC. However, it is not consistent with the experiments of Rieder *et al.* [24]. They observed that an incomplete spindle did *not* inhibit another complete spindle $20\mu m$ away. Furthermore an unattached kinetochore was found to inhibit anaphase onset everywhere within its local spindle even those parts more than $20\mu m$ away. These findings are clearly incompatible with models where inhibition propagates purely diffusively away from incomplete kinetochores into the cytoplasm.

These observations motivate us to consider mechanisms in which the spindle itself plays an active role. If the signal is propagated within the spindle itself, and not spread throughout the cytoplasm, then the obvious transport mechanism is via molecular motors. Propagation via active transport along microtubules is fast; motors can move at speeds of microns per second [35]. As the typical spindle length scale is approximately $10\mu m$, then transport across the spindle takes only seconds at that speed, consistent with rapid checkpoint switch-on/off. Of course, by definition, an unattached kinetochore is not connected via microtubules to a spindle pole. Hence that kinetochore must first produce a freely diffusing species to carry the signal as before. This inhibitory species, which we denote by g^*, initially diffuses through the cytoplasm, but only until it either encounters a minus-end directed microtubule-bound molecular motor, or decays to an inactive form, g. If the molecule encounters a microtubule-bound motor, this binding then stabilises the active g^* form and transports the inhibitory signal to a spindle pole.

However, before we can conclude that this model with active transport is consistent with the experimental data of Rieder *et al.* [24], we need to demonstrate that it is possible to find a lifetime for the g^* that is long enough to allow it to encounter a motor but short enough to prevent more than a small fraction diffusing $20\mu m$ away. If g^* is manufactured at a rate J_{g*} at unattached kinetochores and decays at a rate α_{g*}, then the concentration $c_{g*}(\mathbf{r}, t)$ satisfies the partial differential equation

$$\frac{\partial c_{g*}}{\partial t} = D\nabla^2 c_{g*} - \alpha_{g*} c_{g*} + J_{g*}\delta^3(r). \tag{7}$$

We solve Eq. **7** at steady state, after assuming spherical symmetry around the source (the kinetochore) and negligible concentration of g^* at large distances from the source. The solution is

$$c_{g*}(r) = (J_{g*}/4\pi)(\lambda/r)\exp(-r/\lambda), \tag{8}$$

where $\lambda = \sqrt{D/\alpha_{g*}}$ and r is the distance from the kinetochore. Of course, the assumption of spherical symmetry is a gross approximation, especially as the kinetochore is a plate shaped structure. However, we are only interested

in qualitative results for which this approximation will be reasonable at large distances. If we set the cytoplasmic g^* lifetime to be $\alpha_{g*}^{-1} = 0.5$s, then even with a large diffusion constant of $D = 20\mu\text{m}^2\text{s}^{-1}$, $\lambda \sim 3\mu\text{m}$. Hence the signal $20\mu\text{m}$ away will be greatly attenuated. Due to the short lifetime of the g^* form, the inhibitor forms a steep gradient inside the cell. Hence we predict that subcellular concentration gradients, already believed to be important for microtubule growth and kinetochore capture, also play an important role in checkpoint function [36].

When we considered diffusive sequestration in the previous section we found kinetochore fluxes on the order of 100 molecules/s. If we assume a similar flux $J_{g*} = 100/$s then the concentration of g^* $1\mu\text{m}$ away from the source is approximately $20\mu\text{m}^{-3}$. At this concentration the reaction rate per motor is $20k$, where k is the reaction rate between a pair of proteins. If, as in the previous section, we take $k = 10^{-2}\mu\text{m}^3\text{s}^{-1}$ [34], then we have a rate per motor complex of 0.2s^{-1}. Thus a motor will pick up a g^* molecule within a few seconds if it is close to an unattached kinetochore. If we assume a motor density of $10\mu\text{m}^{-1}$, moving at $1\mu\text{m s}^{-1}$, then we expect a rate on to a spindle pole of perhaps 5s^{-1} per microtubule. Metazoan cells will have large numbers of spindle microtubules in the vicinity of an unattached kinetochore, increasing the on-rate still further. Even if some of the signal is lost in transit to the spindle pole, the flux is adequate to communicate the state of the kinetochore. Note that the localization of the inhibitory signal means that less amplification is needed: the flux off the kinetochore together with directed transport are by themselves sufficient to produce good inhibition. The next question is how the pole processes this information. One attractive possibility is that the g^* inhibit the spindle pole and are subsequently released back into the cytoplasm in the inactive g form. When the last kinetochore attaches, the active transport "wait anaphase" signal is switched off, releasing the inhibition and allowing the spindle pole to broadcast a "go anaphase" signal. This signal could be actively transported by plus end directed motors to communicate with connected kinetochores on the same spindle. However, in the experiments of Ref. [24], once one spindle had entered anaphase, the other spindle also progressed to anaphase regardless of whether it contained unattached kinetochores. This finding suggests that a final "go anaphase" signal is transmitted via diffusion.

For active transport models there is little relevant experimental data. As a result, our modelling has inevitably been more speculative and less detailed than for diffusive sequestration models. In particular it is not clear what the signalling molecule g^* might be. Presumably it cannot involve BubR1-Cdc20 or Mad2-Cdc20, as we require a short lifetime in the cytoplasm. Furthermore these molecules are not known to bind to minus-end directed motors. The active transport model nevertheless predicts that the inhibitory signal is propagated away to the spindle pole by a minus-end directed motor. It is tempting to associate the motor protein dynein with this role; however, this assignment is problematic. If dynein were performing this function then inhibition of dynein would effectively switch off the inhibitory active transport "wait anaphase" signal, resulting in anaphase progression. However, experiments have revealed precisely the opposite effect: inhibition of dynein leads to inhibition of cell cycle progression [37]. Furthermore this block was not due to a more general effect of dynein inhibition, as injecting Mad2 antibodies in dynein inhibited cells still led to rapid anaphase entry [37]. Hence, either dynein is not sufficiently inhibited in this experiment, implying that some inhibitory signal can still leak through, or else other motors are involved. Dynein is already known to transport kinetochore components [26, 37]. However, this transport is associated with the removal of Mad2 binding sites at kinetochores once a microtubule has attached [37]. Without these binding sites, Mad2 cannot cycle through a kinetochore. When this removal occurs at the final attached kinetochore, Cdc20 can no longer be sequestered by Mad2, and instead will be free to trigger anaphase progression.

In summary, our active-transport model is consistent with the experimental data of Rieder *et al.*. We can easily find a lifetime for the inhibitory species g^* that is long enough for the g^* to reach an adjacent microtubule, thereby communicating the state of the kinetochore to the spindle pole, but short enough for strong attenuation at another spindle $20\mu\text{m}$ away.

Discussion

In this paper, we have shown that two models with quite different mechanisms: the diffusive reaction cascade model, and a model with active transport, are both possible signalling mechanisms for the SAC. These two models are schematically illustrated in Fig. 2.

Dual Pathways for the Metazoan SAC? One attractive possibility to reconcile the above models and the experimental data is that, in metazoan cells, both mechanisms are used. Interestingly, cells with unattached kinetochores microinjected with Mad2 antibodies prematurely entered anaphase [38]. This procedure will flood the cell with unsequestered Cdc20, while unattached kinetochores will still be signalling a "wait anaphase" signal via the active transport mechanism. The fact that the cell still enters anaphase indicates that an active transport mechanism is
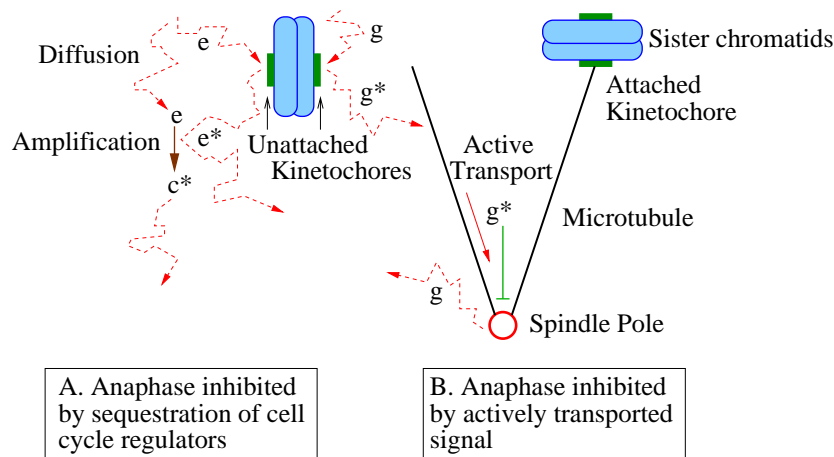
FIG. 2: A schematic of (A) the diffusive two step reaction model and (B) the active-transport model. Kinetochores are shown in green, red dashed lines denote diffusion, and solid red arrows denote motion via active transport. Sister chromatids are shown in blue, while the black lines are microtubules.

probably not essential for checkpoint function: the purely diffusive pathway suffices. On the other hand, the experiments of Rieder *et al.* [24] show that an inhibitory diffusive pathway can be overruled by a second pathway, which, as we have seen, is likely based on active transport. We therefore propose that *either* mechanism can trigger anaphase onset, even without support from the other pathway. The switch off of an active transport based "wait anaphase" signal, or the release of sufficient freely diffusible Cdc20, by switching off an efficient sequestration apparatus, are each separately capable of generating cell cycle progression. With this assumption, our modelling is then entirely consistent with experiment.

Future work Although some of the key principles used by the metazoan SAC are starting to become clear, there is still much that remains to be understood. Even for models of signalling via diffusion, which have been more actively pursued, further quantitative measurements would be very useful. For example, if the *in vivo* diffusion constants were found to be small then this would eliminate some possible models. Also, we predict that amplification without autocatalysis is likely to be required, which implies the existence of at least two inhibiting species (e^*, c^*). Of course, the *in vivo* checkpoint dynamics will likely be much more complicated than our simple outline model, but the requirement for amplification will likely remain. Better characterization of the BubR1/Mad1/Mad2/Cdc20 protein dynamics should therefore allow these predictions to be tested. We would also like to emphasize the close connection between our diffusive two step reaction and other signal cascades, such as for MAPK.

For the alternative active transport pathway, a first goal would be to directly observe and image its components. For example, it would instructive to search for the transport of checkpoint proteins along spindle microtubules *prior* to microtubule attachment. Furthermore, disruption of appropriate minus end motors may be able to generate premature anaphase onset by disrupting the active transport inhibitory signal. As we have discussed previously, it is also important to examine how any such signal is processed by the spindle pole to provide inhibition.

In general, future experimental work will need to measure more of the model parameters before we can make reliable quantitative predictions for intracellular signalling. Nevertheless, as we have shown, computational models can play a useful role in discriminating between viable and inviable mechanisms of checkpoint function.

―――――

[1] Nasmyth, K. (2005) *Cell* **120**, 739-746.
[2] Musacchio A. & Hardwick, K. G. (2002) *Nat. Rev. Mol. Cell Biol.* **3**, 731-741.
[3] Rieder, C. L., Cole, R. W., Khodjakov, A. & Sluder, G. (1995) *J. Cell Biol.* **130**, 941-948.
[4] Rieder, C. L., Schultz, A., Cole, R. & Sluder, G. (1994) *J. Cell Biol.* **127**, 1301-1310.
[5] Castro, A., Bernis, C., Vigneron, S., Labbé, J.-C. & Lorca, T. (2005) *Oncogene* **24**, 314-325.
[6] Howell, B. J., Moree, B., Farrar, E. M., Stewart, S., Fang, G. & Salmon, E. D. (2004) *Curr. Biol.* **14**, 953-964.

[7] Antoni, A. D., Pearson, C. G., Cimini, D., Canman, J.C., Sala, V., Nezi, L., Mapelli, M., Sironi, L., Faretta, M., Salmon, E. D. & Musacchio, A. (2005) *Curr. Biol.* **15**, 214-225.

[8] DeAntoni, A., Sala, V. & Musacchio, A. (2005) *Phil. Trans. R. Soc. B* **360**, 637-648.

[9] Shah, J. V., Botvinick, E., Bonday, Z., Furnari, F., Berns, M. & Cleveland, D. W. (2004) *Curr. Biol.* **14**, 942-952.

[10] Sironi, L., Mapelli, M., Knapp, S., Antoni, A. D., Jeang, K.-T. & Musacchio, A. (2002) *EMBO J.* **21**, 2496-2506.

[11] Luo, X., Tang, Z., Rizo, J. & Yu, H., (2002) *Mol. Cell* **9**, 59-71.

[12] Xia, G., Luo, X., Habu, T., Rizo, J. & Yu, H. (2004) *EMBO J.* **23**, 3133-3143.

[13] Mapelli, M., Filipp, F. V., Rancati, G., Massimiliano, L., Nezi, L., Stier, G., Hagan, R. S., Confalonieri, S., Piatti, S., Sattler, M. & Musacchio, A. (2006) *EMBO J.* **25**, 1273-1284.

[14] Tang, Z., Bharadwaj, R., Li, B. & Yu, H. (2001) *Dev. Cell* **1**, 227-237.

[15] Fang, G. (2002) *Mol. Biol. Cell* **13**, 755-766.

[16] Tang, Z., Shu, H., Oncel, D., Chen, S. & Yu, H. (2004) *Mol. Cell* **16**, 387-397.

[17] Pan, J. & Chen, R.-H. (2004) *Genes Dev.* **18**, 1439-1451.

[18] Sudakin, V., Chan, G. K. T. & Yen, T. J. (2001) *J. Cell Biol.* **154**, 925-936.

[19] Kraft, C., Herzog, F., Gieffers, C., Mechtler, K., Hagting, A., Pines, J. & Peters, J.-M. (2003) *EMBO J.* **22**, 6598-6609.

[20] Acquaviva, C., Herzog, F., Kraft, C. & Pines, J. (2004) *Nat. Cell Biol.* **6**, 892-898.

[21] Doncic, A., Ben-Jacob, E. & Barkai, N. (2005) *Proc. Natl. Acad. Sci. USA* **102**, 6332-6337.

[22] Heinrich, R., Neel, B.G. & Rapoport, T.A. (2002) *Mol. Cell* **9**, 957-970.

[23] Kholodenko, B.N. (2006) *Nat. Rev. Mol. Cell Biol.* **7**, 165-176.

[24] Rieder, C. L., Khodjakov, A., Paliulis, L. V., Fortier, T. M., Cole, R. W. & Sluder, G. (1997) *Proc. Natl. Acad. Sci. USA* **94**, 5107-5112.

[25] McEwen, B. F. Ding, Y. & Heagle, A. B. (1998) *Chromosome Res.* **6**, 123-132.

[26] Howell, B. J., Hoffman, D. B., Fang, G., Murray, A. W. & Salmon, E. D. (2000) *J. Cell Biol.* **150**, 1233-1249.

[27] Clute, P. & Pines, J. (1999) *Nat. Cell Biol.* **1**, 82-87.

[28] Wojcieszyn, J. W., Schlegel, R. A., Wu, E.-S. & Jacobson, K. A. (1981) *Proc. Natl. Acad. Sci USA* **78**, 4407-4410.

[29] Lang, I., Scholz, M. & Peters, R. (1986) *J. Cell Biol.* **102**, 1183-1190.

[30] Seksek, O., Biwersi, J. & Verkman, A. S. (1997) *J. Cell Biol.* **138**, 131-142.

[31] Schmiedeberg, L., Weisshart, K., Diekmann, S., Hoerste, G. M. Z. & Hemmerich, P. (2004) *Mol. Biol. Cell* **15**, 2819-2833.

[32] Berg, H. C. (1993) *Random Walks in Biology*, (Princeton University Press, Princeton), pp. 28.

[33] Vink, M., Simonetta, M., Transidico, P., Ferrari, K., Mapelli, M., De Antoni, A., Massimiliano, L., Ciliberto, A., Faretta, M., Salmon, E. D. & Musacchio, A. (2006) *Curr. Biol.* **16**, 755-766.

[34] Northrup, S. H. & Erickson, H. P., (1992) *Proc. Natl. Acad. Sci. USA* **89**, 3338-3342.

[35] Howard, J. (2001) *Mechanics of Motor Proteins and the Cytoskeleton* (Sinauer Associates, Sunderland, MA).

[36] Wollman, R., Cytrynbaum, E. N., Jones, J. T., Meyer, T., Scholey, J. M. & Mogilner, A. (2005) *Curr. Biol.* **15**, 828-832.

[37] Howell, B. J., McEwen, B. F., Canman, J. C., Hoffman, D. B., Farrar, E. M., Rieder, C. L. & Salmon, E. D. (2001) *J. Cell Biol.* **155**, 1159-1172.

[38] Gorbsky, G. J., Chen, R.-H. & Murray, A. W. (1998) *J. Cell Biol.* **141**, 1193-1205.